Peer-reviewed version available at *Materials* **2020**, *13*, 890; doi:10.3390/ma13040890

# Synthesis of ZnO-NPs Using Convolvulus Leaf Extract and Proving Its Efficiency as an Inhibitor for Carbon Steel Corrosion in 1M HCl

Ghadah M. Al-Senani

*Department of Chemistry, College of Science, Princess Nourah bint Abdulrahman University, Riyadh, Saudi Arabia*

E-mail: gmalsnany@pnu.edu.sa.

## Abstract

This paper studies the use of zinc oxide nanoparticles (***ZnO-NPs***) synthesized using an extract of convolvulus leaves and expired $ZnCl_2$, as an efficient inhibitor for carbon steel corrosion in 1M HCl solution. ***ZnO-NPs*** are characterized by Fourier-transform infrared spectrophotometer (FTIR) and UV–Vis analysis. The technique of weight loss, potentiodynamic polarization, and electrochemical impedance spectroscopy (EIS) has also been used to investigate the prevention of carbon steel corrosion in 1M HCl. The results showed that the efficiency of restraint increased when the concentration of ***ZnO-NPs*** was raised to 91% and that the inhibition efficiency is still high despite its decrease at high temperature, and it acts as a mixed-type inhibitor A sample of carbon steel with the protective inhibitor layer on top was immersed for 20 hours and observed; an increase in the charge transfer resistance (Rct) and stability of the inhibitor was noticed after 6 hours. Adsorption isotherm models demonstrated that the inhibitor adsorption mechanism on the carbon steel surface followed Langmuir, more than Freundlich and Temkin, behavior. The thermodynamic parameters showed that the adsorption process is a mixed adsorption, spontaneous, and exothermic. The results illustrated that the acid medium was a strong inhibitor of carbon steel corrosion. Scanning electron microscope (SEM) showed that the ***ZnO-NPs*** formed a good protective film on the carbon steel surface.

**Keywords:** ZnO-NPs; corrosion; synthesis; carbon steel; convolvulus; leaf; extract

## Introduction

Carbon steel is an engineering material widely used in many industrial applications like manufacturing, construction, defense, transportation, medicine, etc., The corrosion of carbon steel

Peer-reviewed version available at Materials 2020, 13, 890; doi:10.3390/ma13040890

is due to the result of chemical or electrochemical reactions with the surrounding environment, and is a spontaneous process [1]; this can affect the strength of materials, the environment and the safety of society if no precautionary measures are taken to prevent or control it [2]. Corrosion of carbon steel may be present in different forms such as uniform corrosion, galvanic corrosion, pitting corrosion, crevice corrosion, stress corrosion cracking, erosion corrosion, microbial corrosion, and other types.

One of the many traditional techniques available to prevent or control the corrosion of carbon steel is by enhancing its corrosion resistance properties, which is done by the use of suitable inhibitors in the corrosion environment.

A recent development is the use of environment friendly inhibitors. Most natural products are non-toxic, biodegradable and inexpensive. Plant extracts contain many organic compounds that have the ability to inhibit corrosion [3].

Nanotechnology is one of the most active fields of research in modern materials science. Lately, the focus has been on designing and developing the biochemistry of nanoparticles using many plant extracts. Typically, they contain compounds that include electron-rich atoms similar to those found in chemical corrosion inhibitors that are also capable of forming nanoparticles of minerals, which provide more surface area for interaction on the carbon steel surface [4].

This research intends to use expired zinc chloride with an extract of convolvulus leaves in the synthesis of zinc oxide nanoparticles, and to test its effectiveness as a corrosion inhibitor for carbon steel in 1M HCl.

## Experiment

### Materials

All the chemicals used in this study were of analytical grade. HCl (98%) and $ZnCl_2$ (90%) were purchased from Sigma-Aldrich (Germany).

### Preparation of the convolvulus extract

Fresh leaves from the convolvulus plant were collected, washed and dried in the oven for two days at 50 °C and then cut into small pieces and stored in a glass vessel for eventual use.

The extraction was performed by adding 5 g of convolvulus leaves to 100 mL of distilled water in a 250 mL conical flask, stirred for 30 m and heated (60 °C); it was then cooled and filtered

through a Whatman No.1 filter paper. The freshly prepared aqueous extract was used immediately after filtration.

**Synthesis of ZnO-NPs**

The extract from convolvulus leaves (5 ml) was added to 45 ml of $ZnCl_2$ (0.1M). The solution was stirred for 30 minutes at room temperature leading to a change in its color, confirming the formation of ***ZnO-NPs***. It was then separated from the solution by a centrifuge, dried and retained for later use.

**Preparation of the test solution**

The 1 M hydrochloric acid solution was prepared by diluting 37% HCl with double distilled water. 300 mg of the ***ZnO-NPs*** powder was then mixed with 100 mL of 1M HCl and kept as stock solution. All experiments, both in the presence and absence of different concentrations of the inhibitor ranging from 0.006 to 0.12 mg/ml were carried out with this 1M HCl solution.

**Preparation of carbon steel specimens**

The sample of carbon steel used for this study was API X65 from SABIC in Saudi Arabia. The chemical composition of this carbon steel is listed in Table 1. Specimen samples were cut as cylinders having 1 $cm^2$ diameter and inserted in a Teflon holder. They were then polished with 800, 1000 and 1500 grade of emery papers, cleaned with acetone, washed with double distilled water and dried.

**ZnO-NPs characterization**

FT-IR spectra have been taken for dried nanoparticles, performed by a Fourier-transform infrared spectrophotometer (type spectrum 100 FT-IR spectrometer) over a wavenumber range of 400 to 4000 $cm^{-1}$. UV–Vis analysis was done by ultraviolet spectrum (type V-770 UV-Visible/NIR spectrophotometer) over a wavelength range of 200 to 800 nm.

**Surface characterization**

After immersion in 1M HCl, the morphology of the carbon steel surface was studied, both in the presence and absence of 0.06 mg/ml of ***ZnO-NPs*** for 3 h at room temperature using a JSM-

Preprints (www.preprints.org) | NOT PEER-REVIEWED | Posted: 12 January 2020 doi:10.20944/preprints202001.0118.v1

Peer-reviewed version available at Materials 2020, 13, 890; doi:10.3390/ma13040890

6380 LA model scanning electron microscope at a high resolution of 3.0 nm and an accelerating voltage of 0.5 to 30 kV.

**Electrochemical measurements**

The Gill AC apparatus was used to conduct potentiodynamic polarization and electrochemical impedance spectroscopy (EIS) measurements. All measurements were performed using three electrodes: the carbon steel electrode (working electrode), the graphite electrode (counter electrode) and the silver/silver chloride electrode (reference electrode). The working electrode was immersed in a test solution of 1 M HCl with and without 0.006, 0.03, 0.06, 0.09, 0.12 mg/ml of the inhibitor at a temperature of 298 K and 333 K; the open circuit potential was measured after 15 minutes on attaining a steady state. Potentiodynamic polarization measurements were conducted at a scan rate of 0.2 mV $s^{-1}$ and a range of ± 250 mV with respect to its potential to corrode. The frequency range of EIS measurements was between 0.01 and 10000 Hz. The inhibition efficiency ($E_{inh}$%) is calculated using the following equations:

$$E_{inh}\% = \frac{(I_{corr} - I_{corr(inh)})}{I_{corr}} \times 100 \quad (1)$$

$$E_{inh}\% = \frac{(R_{ct(inh)} - R_{ct})}{R_{ct(inh)}} \times 100 \quad (2)$$

where $I_{corr}$ and $I_{corr(inh)}$ are the densities of the corrosion current without and with the inhibitor respectively; this is determined from the intercept of the cathodic and anodic Tafel slopes, $R_{ct}$ and $R_{ct(inh)}$ referred to as the charge transfer resistance without and with the addition of the inhibitor, respectively.

**Weight loss method**

Carbon steel specimens were completely immersed in 50 mL of 1M HCl solution with and without 0.06 mg/ml of the inhibitor for 3 h. The specimens were then washed, dried and weighed. The corrosion rates ($C_{rate}$), degree of surface coverage (θ), and the inhibition efficiency ($E_{inh}$%) of the inhibitor were calculated from the loss in weight using the following equations:

$$C_{rate} = \frac{W}{At} \quad (3)$$

Preprints (www.preprints.org) | NOT PEER-REVIEWED | Posted: 12 January 2020 doi:10.20944/preprints202001.0118.v1

Peer-reviewed version available at Materials 2020, 13, 890; doi:10.3390/ma13040890

$$\theta = \frac{(W_0 - W_{inh})}{W_0} \quad (4)$$

$$E_{inh}\% = \frac{(W_0 - W_{inh})}{W_0} \times 100 \quad (5)$$

where W is weight loss of carbon steel, A ($cm^2$) is the area of specimens, t (h) is the immersion time, and $W_o$ and $W_{inh}$ are the losses in weight (mg) of carbon steel.

## Results and Discussion

### *Characterization of ZnO-NPs*

Analysis of the FTIR and UV spectra of ***ZnO-NPs*** shown in Figure 1 shows that there was a peak at 501 $cm^{-1}$ illustrated by UV spectrum (280 nm), as evidence of the presence of ***ZnO-NPs***. Meanwhile, the peaks in 3904, 3586, 3510, 1926, 1608, 1409 and 1013 $cm^{-1}$ were attributed to the functional groups in the convolvulus leaf extract [5-7].

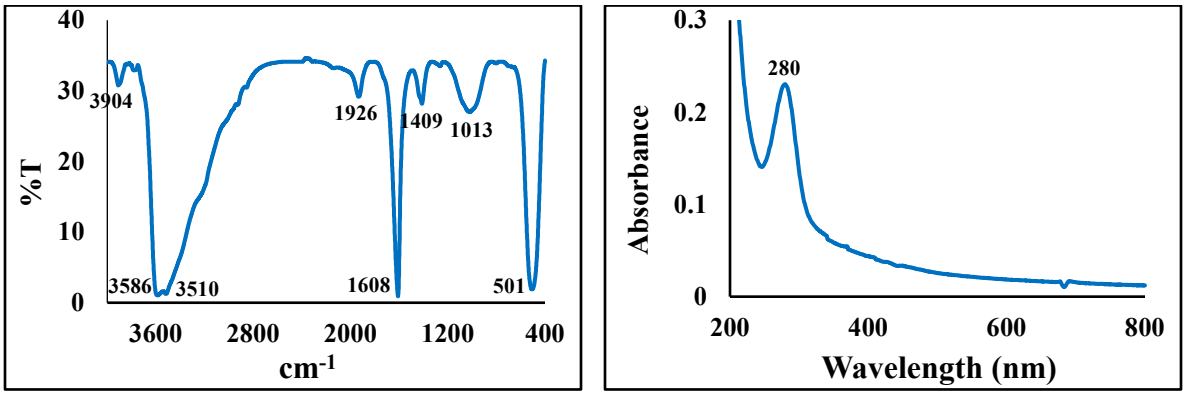


Figure 1. FTIR and UV–Vis of ZnOGNPs.

### *Weight loss method*

Weight loss measurements were applied to evaluate the efficiency of the inhibitor, both in the presence and absence of different concentrations of ***ZnO-NPs***. The carbon steel electrodes were immersed for up to 3 h at a temperature of 298 K and 333 K. Figure 2 illustrates that the inhibition efficiency increases with an increase in the inhibitor concentration, and becomes stable after 0.06% concentration. Table 1 shows the results obtained, proving that the inhibitor molecules adsorb on the active surface sites of carbon steel that was saturated with inhibitor molecules preventing continued corrosion [2, 8, 9].

Preprints (www.preprints.org) | NOT PEER-REVIEWED | Posted: 12 January 2020 doi:10.20944/preprints202001.0118.v1

Peer-reviewed version available at Materials 2020, 13, 890; doi:10.3390/ma13040890

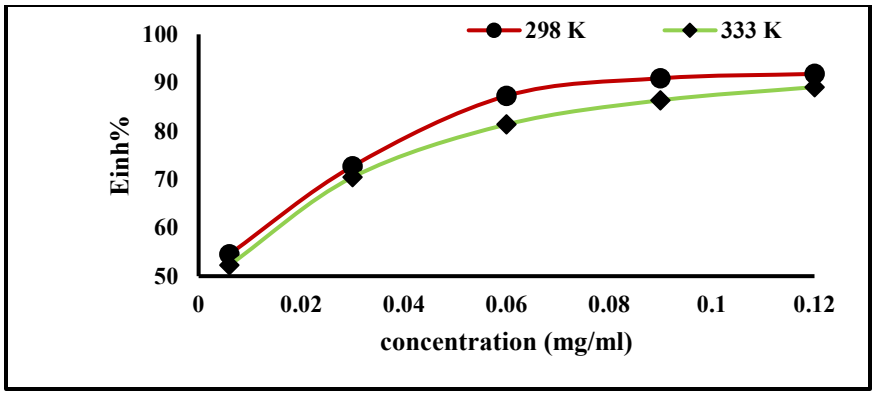


**Figure 2.** Effect of ZnO-NPs concentrations on inhibition efficiency ($E_{inh}$%) of carbon steel in 1 M HCl at 298 and 333 K.

**Table 1.** The values of $C_{rate}$, and $E_{inh}$% for different ZnO-NPs concentrations at 298 and 333 K in 1M HCl solution.

| Temperature | 298 K | | 333 K | |
|---|---|---|---|---|
| Concentration (mg/ml) | $C_{rate}$ (mg/cm$^2$.h) | $E_{inh}$% | $C_{rate}$ | $E_{inh}$% |
| Blank | 1.14 | - | 5.72 | - |
| 0.006 | 0.52 | 54.55 | 2.73 | 52.27 |
| 0.03 | 0.21 | 81.82 | 1.43 | 75.00 |
| 0.06 | 0.16 | 86.36 | 1.07 | 81.36 |
| 0.09 | 0.10 | 90.91 | 0.78 | 86.36 |
| 0.12 | 0.09 | 91.82 | 0.62 | 89.09 |

### *Electrochemical measurements*

### Potentiodynamic polarization measurements

Figure 3 illustrates the potentiodynamic polarization curves for both the anodic and cathodic Tafel behavior of carbon steel corrosion in 1M HCl, in the absence and presence of different concentrations of the inhibitor at a temperature of 298 K and 333 K. The Tafel slopes show that the addition of an inhibitor influences both anodic and cathodic reactions leading to the conclusion that the effect of ***ZnO-NPs*** inhibitors are a mixed-type. A clear displacement of the Tafel anodic and cathodic curves has been observed with an increase in the ***ZnO-NPs*** concentration to 0.06mg/ml and above, at which point the inhibitor effect becomes almost constant due to the saturation of carbon steel surface with the inhibitor molecules [10]. It should be noted that as the concentration of the inhibitor increased, the rate of corrosion decreased. This means

Preprints (www.preprints.org) | NOT PEER-REVIEWED | Posted: 12 January 2020 doi:10.20944/preprints202001.0118.v1

Peer-reviewed version available at Materials 2020, 13, 890; doi:10.3390/ma13040890

that the inhibitor has a high efficiency of 91% at a concentration of 0.12 mg/ml at 298 K, as recorded in Table 2. The high temperature has increased the $I_{corr}$ [11], but the effect of the inhibitor remains the same at a temperature of 298 K. Its effect at a temperature of 333 K has almost become constant after 0.06 mg/ml concentration of ***ZnO-NPs*** concluding that even at high temperatures [10], when the surface of the electrode is saturated with inhibitor molecules [12], the inhibition mechanism remains constant.

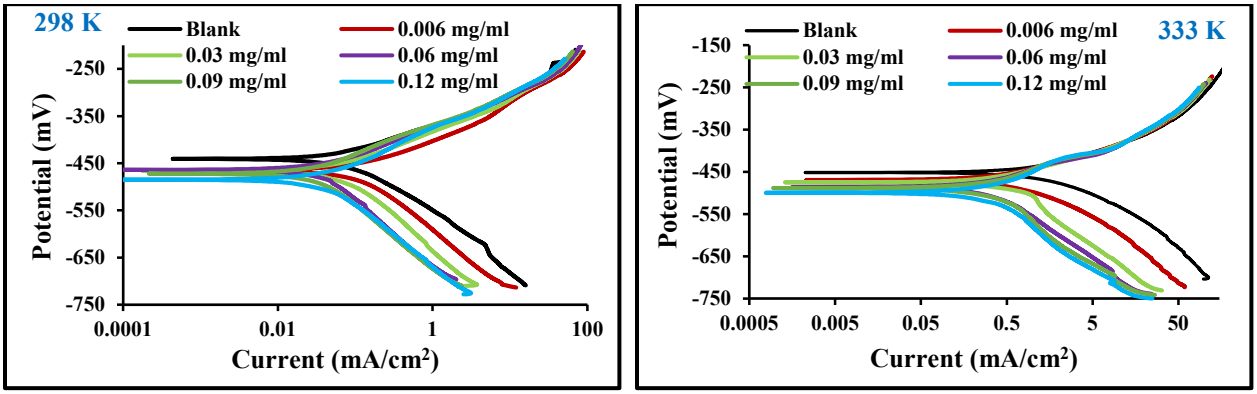


**Figure 3.** Polarization curves for carbon Steel in 1 M HCl with and without different concentrations of ZnO-NPs at 298 and 333 K.

**Table 2.** Potentiodynamic polarization parameters

| Concentration (mg/ml) | 298 K | | | | | 333 K | | | | |
|---|---|---|---|---|---|---|---|---|---|---|
| | $E_{corr}$ (mV) | $\beta_a$ (mA/cm²) | $\beta_c$ (mA/cm²) | $I_{corr}$ (mA/cm²) | η% | - $E_{corr}$ (mV) | $\beta_a$ (mA/cm²) | $\beta_c$ (mA/cm²) | $I_{corr}$ (mA/cm²) | η% |
| 0 | - 441.01 | 76.90 | 123.28 | 5.15 | 0 | 451.83 | 109.87 | 150.38 | 9.93 | 0 |
| 0.006 | - 464.22 | 70.78 | 133.75 | 2.235 | 56.60 | 468.61 | 91.34 | 147.17 | 4.29 | 58.35 |
| 0.03 | - 466.08 | 69.55 | 144.68 | 1.02105 | 80.17 | 480.03 | 71.25 | 145.87 | 2.37 | 77.02 |
| 0.06 | - 464.29 | 67.06 | 145.97 | 0.6659 | 87.07 | 486.48 | 67.38 | 143.65 | 1.78 | 82.76 |
| 0.09 | - 473.69 | 65.83 | 147.10 | 0.495 | 90.39 | 491.62 | 66.73 | 137.29 | 1.39 | 86.55 |
| 0.12 | - 484.89 | 68.11 | 136.95 | 0.45 | 91.26 | 511.89 | 64.75 | 132.25 | 1.09 | 89.47 |

**Electrochemical impedance measurements**

Figure 4 illustrates the application of electrochemical impedance technique to determine the corrosion behavior of carbon steel in 1 M HCl with the absence and presence of ***ZnO-NPs*** at a temperature of 298 K and 333 K using electrochemical impedance spectroscopy (EIS). On the

Preprints (www.preprints.org) | NOT PEER-REVIEWED | Posted: 12 January 2020 doi:10.20944/preprints202001.0118.v1

Peer-reviewed version available at Materials 2020, 13, 890; doi:10.3390/ma13040890

Nyquist diagram of 1M HCl compared with different concentrations of ***ZnO-NPs*** and blank solution, it can be seen that all curves follow the behavior of the blank solution. The electrochemical impedance diagram shows the presence of a small diameter semicircle in the blank solution that increases with the presence of the inhibitor as well as with the increased concentration. This means that the corrosion mechanism did not change even with the inhibitor [13].

The results in Table 3 show that the double layer capacity ($C_{dl}$), charge transfer resistance ($R_{ct}$) and solution resistance ($R_s$) gradually increased with an increase in the inhibitor concentration, and the corrosion rate became very low compared to the blank solution even with low concentrations. This shows that the inhibitor has a strong influence on the corrosion of carbon steel [14].

The Bode and phase angle diagrams showed an increased area under the curves in the presence of the inhibitor compared to a blank solution. The corrosion resistance may significantly be increased with an increase in the quantity and concentration of the inhibitor [15].

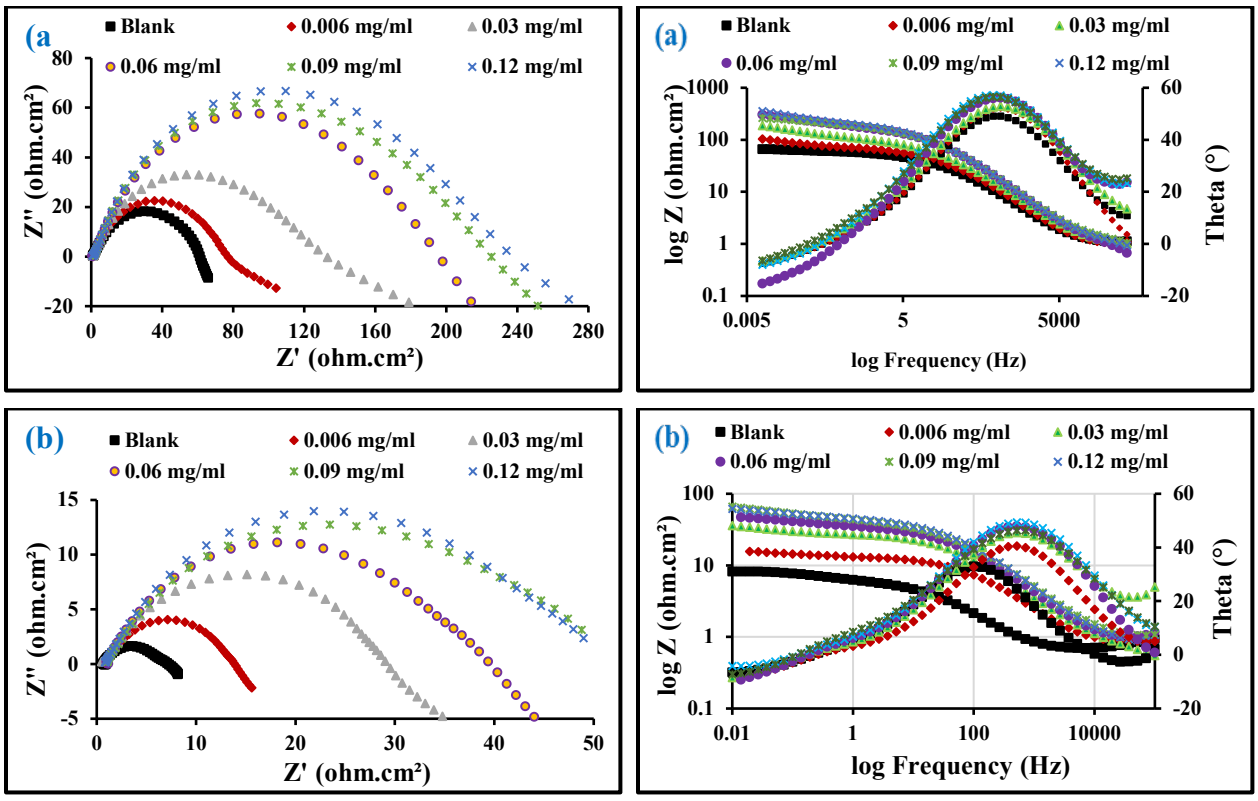


**Figure 4.** EIS digrams for carbon Steel in 1 M HCl with and without different concentrations of ZnO-NPs at (a) 298 and (b) 333 K.

**Table 3.** EIS parameters

Preprints (www.preprints.org) | NOT PEER-REVIEWED | Posted: 12 January 2020 doi:10.20944/preprints202001.0118.v1

Peer-reviewed version available at Materials 2020, 13, 890; doi:10.3390/ma13040890

| Concentration (mg/ml) | 298 K | | | | | 333 K | | | | |
|---|---|---|---|---|---|---|---|---|---|---|
| | Rs (ohms.cm$^2$) | Rct (ohms.cm$^2$) | Cdl (mF) | $I_{corr}$ (mA/cm$^2$) | η% | Rs (ohms.cm$^2$) | Rct (ohms.cm$^2$) | Cdl (mF) | $I_{corr}$ (mA/cm$^2$) | η% |
| 0 | 0.29 | 21.55 | 0.56 | 1.21 | - | 0.70 | 5.73 | 7.33 | 4.56 | - |
| 0.006 | 0.32 | 55.48 | 0.47 | 0.35 | 61.16 | 0.85 | 12.58 | 1.00 | 2.07 | 54.45 |
| 0.03 | 0.41 | 127.00 | 0.43 | 0.21 | 81.26 | 0.89 | 27.86 | 0.85 | 0.94 | 79.43 |
| 0.06 | 0.43 | 191.30 | 0.36 | 0.14 | 88.73 | 0.91 | 35.61 | 0.63 | 0.73 | 83.91 |
| 0.09 | 0.68 | 220.10 | 0.36 | 0.12 | 90.21 | 0.92 | 45.34 | 0.54 | 0.58 | 87.36 |
| 0.12 | 0.81 | 226.70 | 0.30 | 0.11 | 90.49 | 0.94 | 59.48 | 0.52 | 0.44 | 90.37 |

### *Effect of immersion time*

EIS was applied to determine the stability of ***ZnO-NPs*** with immersion time. The EIS technique studies the resistance of the electrode to corrosion without any influence on its behavior; hence, it is considered an appropriate technique for testing immersion time. In Figure 5, we observe the response of steel to corrosion in 1M HCl in the presence of 0.06 mg/ml of the ***ZnO-NPs*** at different immersion durations at a temperature of 298 K. It is clear from Figure 5 that the increase in immersion time does not affect the corrosion process mechanism [16]. It was observed that the diameter of the semicircle in the Nyquist plots increases with an increase in immersion time. The important EIS parameters are listed in Table 4 that make it clear that $R_{ct}$ increases with an increased immersion time, indicating the decreased corrosion rate. Thus, the prolonged immersion time increases the adsorption of ***ZnO-NPs*** molecules on the carbon steel surface, ensuring its stability. It was observed that the surface coverage became stable after approximately 6 hours [17, 18].

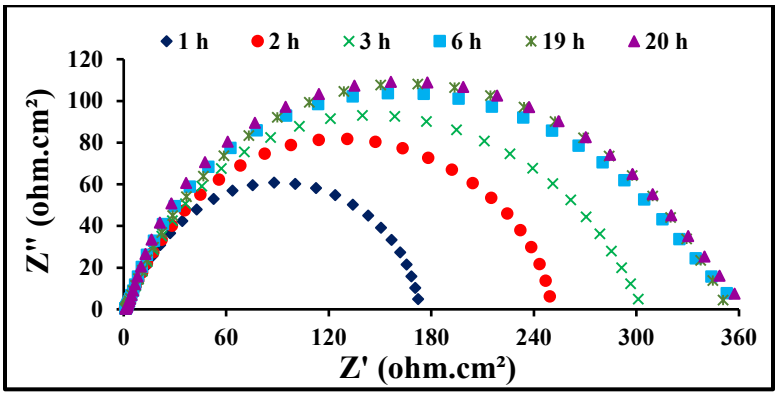


**Figure 5.** Nyquist plots for carbon Steel in 1M HCl with 6 mg/ml of ZnO-NPs at 298 K.

**Table 4.** EIS parameters

Preprints (www.preprints.org) | NOT PEER-REVIEWED | Posted: 12 January 2020 doi:10.20944/preprints202001.0118.v1

Peer-reviewed version available at Materials 2020, 13, 890; doi:10.3390/ma13040890

| Time (h) | 298 K | | |
|---|---|---|---|
| | Rct (ohms.cm$^2$) | Cdl (mF) | $I_{corr}$ (mA/cm$^2$) |
| 1 | 200.0 | 0.53 | 0.130 |
| 2 | 276.4 | 0.49 | 0.094 |
| 3 | 302.0 | 0.32 | 0.087 |
| 6 | 343.4 | 0.30 | 0.076 |
| 19 | 353.0 | 0.29 | 0.074 |
| 20 | 359.3 | 0.28 | 0.072 |

*Adsorption isotherm models and Thermodynamic*

Various adsorption isotherm models such as Langmuir, Freundlich, and Temkin were used to find information about the type of reactions that occurred between carbon steel surfaces and adsorbent molecules of the inhibitor, the adsorption equilibrium constant, and the surface coverage.

The degree of surface coverage was determined from the data of potentiodynamic polarization. The following equations for adsorption isotherm models have been applied to obtain the linear relationship between the degree of surface coverage ($\boldsymbol{\theta}$) and the inhibitor concentration ($\boldsymbol{C_{inh}}$) [19, 20]:

Langmuir: $$\frac{C_{inh}}{\theta} = \frac{1}{K_{ads}} + C_{inh} \quad (6)$$

Freundlich: $$ln\,\theta = ln\,K_{ads} + \frac{1}{n}\,ln\,C_{inh} \quad (7)$$

Temkin: $$\theta = \frac{-ln\,K_{ads}}{2a} - \frac{ln\,C_{inh}}{2a} \quad (8)$$

where $K_{ads}$ is the adsorption equilibrium constant**;** a is the molecular reaction constant that attracts forces if the value is positive and repulses if it is negative; n is a measure of adsorption intensity where, if the value of 1/n lies between 0 and 1 the adsorption of inhibitor molecules on carbon steel surface is easy, equal to 1 is moderate, and more than 1 is difficult.

The adsorption isotherm plots are presented in Figure 6 and linear relationship and parameters obtained from those plots are listed in Table 5. Langmuir isotherm model was the best fit compared to Freundlich and Temkin; where the correlation coefficient ($R^2$) was close to unity. The values of $K_{ads}$ for Langmiur and Frendulich decreases with increase in temperature indicating

Preprints (www.preprints.org) | NOT PEER-REVIEWED | Posted: 12 January 2020 doi:10.20944/preprints202001.0118.v1

Peer-reviewed version available at Materials 2020, 13, 890; doi:10.3390/ma13040890

that the adsorption process slows down with rise in temperature and is unfavorable at higher temperatures. The $K_{ads}$ for Temkin increases with increase in temperature and suggests that the adsorbed inhibitor on metal surface at higher temperatures was physical adsorption [21, 22].

Moreover, the $K_{ads}$, is also used to calculate the values of the standard Gibbs free energy ($\Delta G°_{ads}$) according to the equation given below [23]:

$$\Delta G°_{ads} = -RT\ ln\ (55.5\ K_{ads}) \quad (9)$$

Where R is the universal gas constant, T is the absolute temperature and 55.5 is the molar heat of water adsorption. The negative $\Delta G°_{ads}$ values in Table 2 show that the adsorption of ***ZnO-NPs*** on carbon steel surfaces is highly spontaneous at high temperatures. The values of $\Delta G°_{ads}$ are between -20 and - 41 kJ/mol in the Langumir and Temkin isotherm models, which meant that both chemical and physical adsorption (mixed adsorption) occurred on the carbon steel surface, while it was lower than -20kJ/Mol in the Freundlich isotherm model, which meant that the ***ZnO-NPs*** adsorbed onto the surface of carbon steel was physical adsorption [23, 24]. In general, values of $\Delta G°_{ads}$ less than -20 kJ/mol correspond to electrostatic reactions between the inhibitor molecules and the carbon steel surface (physisorption). Similarly, values that are lower than -40 kJ/mol involve sharing the charge or transfer from inhibitor molecules to the carbon steel surface to form a coordinate bond (chemisorption).

The adsorption enthalpy ($\Delta H°_{ads}$) and the adsorption entropy ($\Delta S°_{ads}$) for ***ZnO-NPs*** adsorbed on the carbon steel surface were calculated from the Gibbs–Helmholtz and Gibbs free energy equations [25, 26]:

$$\frac{\Delta G°_{ads}}{T_2} - \frac{\Delta G°_{ads}}{T_1} = \Delta H°_{ads}\left(\frac{1}{T_2} - \frac{1}{T_1}\right) \quad (10)$$

$$\Delta G°_{ads} = \Delta H°_{ads} - T\Delta S°_{ads} \quad (11)$$

The values of $\Delta H°_{ads}$ and $\Delta S°_{ads}$ are listed in Table 5. The negative values of $\Delta S°_{ads}$ are an indication that corrosion process is controlled by an activation complex [25-27]. The negative value of enthalpies $\Delta H°_{ads}$ reflect the exothermic behavior of the inhibitor on carbon steel surface on the Langmuir and Freundlich isotherms, but is positive on the Temkin isotherm; moreover, the positive value of $\Delta H°_{ads}$ reflects the fact that adsorption process is endothermic [25].

Preprints (www.preprints.org) | NOT PEER-REVIEWED | Posted: 12 January 2020 doi:10.20944/preprints202001.0118.v1

Peer-reviewed version available at Materials 2020, 13, 890; doi:10.3390/ma13040890

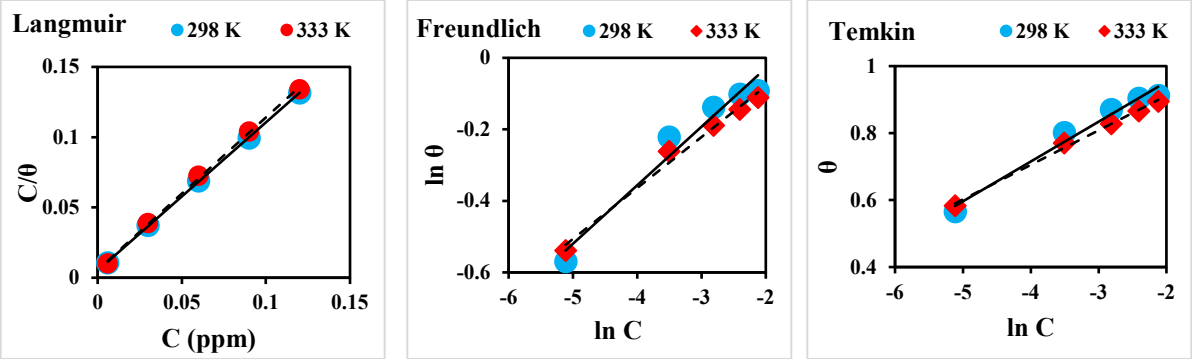


**Figure 6:** Langmuir, Freundlich, Temkin isotherms for the adsorption of ZnO-NPs molecules on the surface of the carbon steel.

**Table 5.** Adsorption isotherm parameters.

| Isotherm models | Temperature | $K_{ads}$ | $R^2$ | $n$ | $a$ | $\Delta G^o$ (kJ/mol) | $\Delta H^o$ (kJ/mol) | $\Delta S^o$ (J/mol K) |
|---|---|---|---|---|---|---|---|---|
| Langmuir | 298 K | 200 | 0.9998 | - | - | - 23.0778 | - 2.66 | - 68.51 |
| | 333 K | 178.57 | 0.9989 | - | - | - 25.4746 | | |
| Freundlich | 298 K | 1.35 | 0.9604 | 0.164 | - | - 10.6899 | - 2.15 | - 28.65 |
| | 333 K | 1.23 | 0.9862 | 0.143 | - | - 11.6902 | | |
| Temkin | 298 K | 22324.87 | 0.9766 | - | - 4.205 | - 34.7599 | 19.22 | - 181.15 |
| | 333 K | 50633.28 | 0.9955 | - | - 4.845 | - 41.1097 | | |

*Scanning electron microscope (SEM)*

The carbon steel surface was studied by a scanning electron microscope after immersing it for 3 h in 1M HCl solution in the absence and presence 0.06 mg/ml of ***ZnO-NPs***. Figure 7 illustrates that carbon steel in the blank solution is highly corrosive as cracks and pits appeared on the surface along with scratches; while in the presence of an inhibitor, corrosion was prevented without pits or cracks on the surface, and very few scratches [28, 29]. Deposits were also observed on the surface resulting in the formation of a protective film on the carbon steel surface. Hence, ***ZnO-NPs*** are an effective inhibitor of corrosion in carbon steel exposed to HCl solutions.

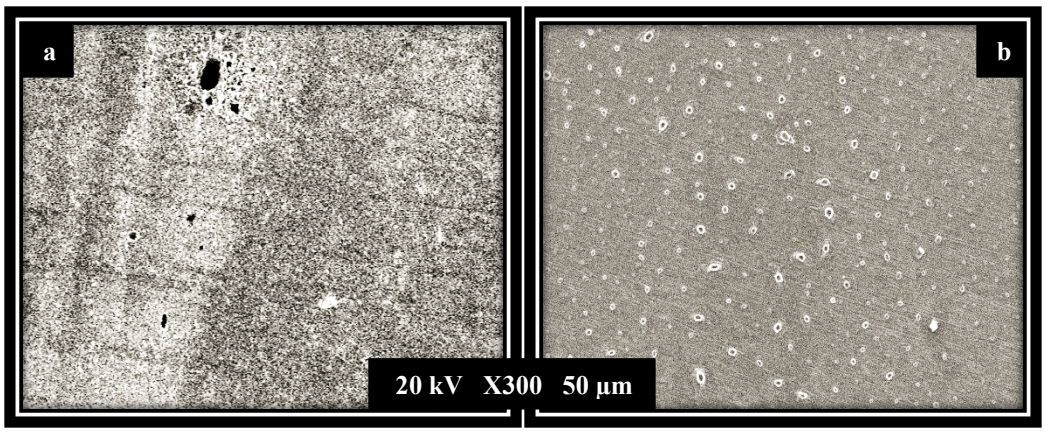


**Figure 7.** SEM images of carbon steel immersed in 1 M HCl (a) and in the presence 10% of inhibitor (b) for 3h at 298 K.

## Conclusion

***ZnO-NPs*** can be prepared by synthesis using expired ZnCl and convolvulus extract. The results obtained from the methods of weight loss, potentiodynamic polarization, and EIS measurements proved that ***ZnO-NPs*** are an effective inhibitor of carbon steel corrosion in 1M HCl. The inhibition efficiency increases with increasing ***ZnO-NPs*** concentration, and decreases at higher temperature. It also works as a mixed type inhibitor. The carbon steel corrosion inhibition process follows the Langmuir isotherm than Freundlich and Temkin isotherms. The calculated values for $\Delta G°_{ads}$, $\Delta H°_{ads}$, and $\Delta S°_{ads}$ showed that the adsorption process was spontaneous and exothermic, and the inhibitor molecules adsorbed on the surface of the metal through chemisorption and physisorption mechanisms (mixed adsorption). The results of the SEM study revealed that the ***ZnO-NPs*** can act as an effective inhibitor of carbon steel corrosion in 1M HCl solutions.

## Acknowledgments

This study was supported by Princess Nourah Bint Abdulrahman University, as a part of the faculty member sabbaticals.

## Reference

1. Tang, L.; Li, X.; Lau, S.; Li, L.; Mu, G.; Liu, G. A Kinetic Model to Study the Corrosion Inhibition of 500µM PAR for Steel Corrosion in 0.5-3.0 M Hydrochloric Acid. Recent Patents on Corrosion Science 2011, 1, 56-62.

2. Sliem, M.; Afifi, M.; Radwan, A.; Fayyad, E.; Shibl, M.; Heakal, F.; Abdullah, A. AEO7 Surfactant as an Eco-Friendly Corrosion Inhibitor for Carbon Steel in HCl solution. Scientific Reports 2019, 9, 2319, DOI:10.1038/s41598-018-37254-7.

1. Bouanisa, M.; Tourabia, M.; Nyassia, A.; Zarroukb, A.; Jamac, C.; Bentiss. F. Corrosion inhibition performance of 2,5-bis(4-dimethylaminophenyl)-1,3,4-oxadiazole for carbon steel in HCl solution: Gravimetric, electrochemical and XPS studies. Applied Surface Science 2016, 389, 952–966.

2. Al-Dahiri, R.; Turkustani, A.; Salam, M. The Application of Zinc Oxide Nanoparticles as An Eco-Friendly Inhibitor for Steel in Acidic Solution. Int. J. Electrochem. Sci. 2020, 15, 442 – 457, DOI: 10.20964/2020.01.01.

3. Zheng, Y.; Fu, L.; Han, F.; Wang, A.; Cai, W.; Yu, G.; Yang, J.; Peng, F. Green biosynthesis and characterization of zinc oxide nanoparticles using *Corymbia citriodora* leaf extract and their photocatalytic activity. Green Chemistry Letters and Reviews 2015, 8, 2, 59–63, http://dx.doi.org/10.1080/17518253.2015.1075069.

4. Soto‐Robles, C.; Nava, O.; Vilchis‐Nestor, A.; Castro‐Beltran, A.; Gomez‐Gutierrez, C.; Lugo‐Medina, E.; Olivas, A.; Luque, P. Biosynthesized zinc oxide using *Lycopersicon esculentum* peel extract for methylene blue degradation. Journal of Materials Science: Materials in Electronics 2018, 29, 3722–3729, https://doi.org/10.1007/s10854-017-8305-4.

5. Rao, M.; Gautam, P. Synthesis and Characterization of ZnO Nanoflowers Using Chlamydomonas reinhardtii: A Green Approach. Environmental Progress & Sustainable Energy 2016, 35, 4, 1020-1026, https://doi.org/10.1002/ep.12315.

6. Ijuo, G.; Chahul, H.; Eneji, I. Kinetic and Thermodynamic Studies of Corrosion Inhibition of Mild Steel using Bridelia ferruginea Extract in Acidic Environment Kinetic and Thermodynamic Studies of Corrosion Inhibition of Mild Steel using Bridelia ferruginea Extract in Acidic Environment. Journal of Advanced Electrochemistry 2016, 2, 3, 107–112.

7. Abeng, F.; Idim, V.; Nna, P. Kinetics and Thermodynamic Studies of Corrosion Inhibition of Mild Steel Using Methanolic Extract of Erigeron floribundus (Kunth) in 2 M HCl Solution. World News of Natural Sciences 2017, 10, 26-38.

8. Ahmed, S.; Ali, W.; Khadom, A. Synthesis and investigations of heterocyclic compounds as corrosion inhibitors for mild steel in hydrochloric acid. International Journal of Industrial Chemistry 2019, 10, 159–173, https://doi.org/10.1007/s40090-019-0181-8.

9. Fiori-Bimbi, M.; Alvarez, P.; Vaca, H.; Gervasi, C. Corrosion inhibition of mild steel in HCL solution by pectin. Corrosion Science 2015, 92, 192–199.

10. Meng, Y.; Ning, W.; Xu, B.; Yang, W.; Zhang, K.; Chen, Y.; Li, L.; Liu, X.; Zheng, J.; Zhang, Y. Inhibition of mild steel corrosion in hydrochloric acid using two novel pyridine Schiff base derivatives: a comparative study of experimental and theoretical results. RSC Advances 2017, 7, 43014–43029.

11. Xu, S.; Zhang, S.; Guo, L.; Feng, L.; Tan, B. Experimental and Theoretical Studies on the Corrosion Inhibition of Carbon Steel by Two Indazole Derivatives in HCl Medium. Materials 2019, 12, 1339, https://doi.org/10.3390/ma12081339.

12. Ahamad, I.; Prasad, R.; Quraishi, M. Thermodynamic, electrochemical and quantum chemical investigation of some Schiff bases as corrosion inhibitors for mild steel in hydrochloric acid solutions. Corrosion Science 2010, 52, 933–942.

13. Quadri, T.; Olasunkanmi, L.; Fayemi, O.; Solomon, M.; Ebenso, E. Zinc Oxide Nanocomposites of Selected Polymers: Synthesis, Characterization, and Corrosion Inhibition Studies on Mild Steel in HCl Solution. ACS Omega 2017, 2, 8421−8437, DOI: 10.1021/acsomega.7b01385.

14. Ahmed, R.; Farghali, R.; Fekry, A. Study for the Stability and Corrosion Inhibition of Electrophoretic Deposited Chitosan on Mild Steel Alloy in Acidic Medium. Int. J. Electrochem. Sci. 2012, 7, 7270 – 7282.

15. Izadi, M.;Shahrabi, T.; Ramezanzadeh B. Active corrosion protection performance of an epoxy coating applied on the mild steel modified with an eco-friendly sol-gel film impregnated with green corrosion inhibitor loaded nanocontainers. Applied Surface Science 2018, 440, 491–505.

16. Usman, B.; Umoren, S.; Gasem, Z. Inhibition of API 5L X60 steel corrosion in CO2-saturated 3.5% NaCl solution by tannic acid and synergistic effect of KI additive. Journal of Molecular Liquids 2017, 237, 146–156.

17. Ituen1, E.; Akaranta, O.; James, A. Evaluation of Performance of Corrosion Inhibitors Using Adsorption Isotherm Models: An Overview. Chemical Science International Journal 2017, 18, 1, 1-34, 2017; Article no.CSIJ.28976.

18. Sophie, P.; Anthony, N. Kinetic, Thermodynamic and Adsorption Studies for Corrosion Inhibition of Carbon Steel by Asparagaeus Setaceus L. + Mn2+ in Neutral Media. International Journal for Research in Applied Science & Engineering Technology 2018, 6, I, 3125-3133, DOI: 10.22214/ijraset.2018.1432.

19. Iroha, N.; Hamilton-Amachree, A. Inhibition and adsorption of oil extract of Balanites aegyptiaca seeds on the corrosion of mild steel in hydrochloric acid environment. World Scientific News 2019, 126, 183-197.

20. Santosa, E.; Cordeiroa, R.; Santosa, M.; Rodriguesb, P.; Singhc, A.; D'Elia, E. Barley Agro-industrial Residues as Corrosion Inhibitor for Mild Steel in 1mol L-1 HCl Solution. Materials Research. 2019, 22, 2, DOI: http://dx.doi.org/10.1590/1980-5373-MR-2018-0511.

21. Al-Senani, G.; Alshabanat, M. Study the Corrosion Inhibition of Carbon Steel in 1 M HCl Using Extracts of Date Palm Waste. Int. J. Electrochem. Sci. 2018, 13, 3777 – 3788, DOI: 10.20964/2018.04.03.

22. Saha, S.; Dutta, A.; Ghosh, P.; Sukul, D.; Banerjee, P. Adsorption and corrosion inhibition effect of Schiff base molecules on the mild steel surface in 1 M HCl medium: a combined experimental and theoretical approach. Phys. Chem. Chem. Phys. 2015, 17, 5679-5690, DOI: 10.1039/C4CP05614K.

23. AL-Senani, G.; AL-Saeedi, S.; AL-Mufarij, R. Coriandrum sativum leaves extract (CSL) as an eco-friendly green inhibitor for corrosion of carbon steel in acidic media. J. Mater. Environ. Sci. 2016, 7, 7, 2240-2251.

24. Odewunmi, N.; Umoren, S.; Gasem, Z. Utilization of watermelon rind extract as a green corrosion inhibitor for mild steel in acidic media. Journal of Industrial and Engineering Chemistry 2015, 21, 239-247, https://doi.org/10.1016/j.jiec.2014.02.030.

25. Nnanna, L.; Uchendu, K.; Nwosu, F.; Ihekoronye, U.; Eti, E. Gmelina Arborea Bark Extracts as a Corrosion Inhibitor for Mild Steel in an Acidic Environment. International Journal of Materials and Chemistry 2014, 4, 2, 34-39, DOI:10.5923/j.ijmc.20140402.03..

26. Zheng, X.; Gong, M.; Li, Q.; Guo, L. Corrosion inhibition of mild steel in sulfuric acid solution by loquat (Eriobotrya japonica Lindl.) leaves Extract. Scientific Reports 2018, 8, 9140, DOI:10.1038/s41598-018-27257-9.

27. Verma, C.; Quraishi, M. Adsorption behavior of 8,9-bis(4 (dimethyl amino) phenyl)benzo[4,5]imidazo[1,2-a]pyridine-6,7- dicarbonitrile on mild steel surface in 1 M HCl. Journal of the Association of Arab Universities for Basic and Applied Sciences 2017, 22, 55–61, https://doi.org/10.1016/j.jaubas.2016.01.003.